



Article

Transcriptional Effects of Rootstock on Scion after Drought: A Case Study of Using *MdGH3* RNAi as the Rootstock

Jieqiang He^{1,2,3} , Junxing Guo^{1,2,3} , Lijuan Jiang^{1,2}, Wenjing An², Fengwang Ma^{1,2}, Qingmei Guan^{1,2,3,*} and Chundong Niu^{1,2,3,*}

¹ State Key Laboratory of Crop Stress Biology for Arid Areas, Yangling, Xianyang 712100, China

² Shaanxi Key Laboratory of Apple, College of Horticulture, Northwest A&F University, Yangling, Xianyang 712100, China

³ Shenzhen Research Institute, Northwest A&F University, Shenzhen 518000, China

* Correspondence: qguan@nwafu.edu.cn (Q.G.); niuchundong@163.com (C.N.)

Abstract: Drought stress is an important environmental factor limiting apple yield and fruit quality. Previously, we identified GRETCHEN HAGEN3.6 (GH3.6) as a negative regulator of drought stress in apple trees. Using transgenic *MdGH3* RNAi (knocking down *MdGH3.6* and its five homologs) plants as rootstock can increase drought tolerance, water use efficiency, flowering, and fruit quality of the Fuji scion after drought stress. However, the molecular mechanism behind this phenomenon is still unknown. Here, we performed transcriptome sequencing of the grafted plants (Fuji/GL-3 where Fuji was used as the scion and non-transgenic GL-3 was used as the rootstock, and Fuji/*MdGH3* RNAi where *MdGH3* RNAi was used as the rootstock) under control and drought conditions. Under control conditions, 667 up-regulated genes and 176 down-regulated genes were identified in the scion of Fuji/*MdGH3* RNAi, as compared to the scion of Fuji/GL-3. Moreover, 941 up-regulated genes and 2226 down-regulated genes were identified in the rootstock of *MdGH3* RNAi plants relative to GL-3. GO terms of these differentially expressed genes (DEGs) in scion and rootstock showed associations with plant growth, fruit development, and stress responses. After drought stress, 220 up-regulated and 452 down-regulated genes were identified in *MdGH3* RNAi rootstock, as compared to GL-3. Significantly enriched GO terms included response to abiotic stimulus, cell division, microtubule-based process, metabolic and biosynthetic process of flavonoid, pigment, and lignin. The comparison between the scion of Fuji/*MdGH3* RNAi and Fuji/GL-3 yielded a smaller number of DEGs; however, all of them were significantly enriched in stress-related GO terms. Furthermore, 365 and 300 mRNAs could potentially move from *MdGH3* RNAi rootstock to scion under control and drought conditions, respectively, including FIDDLEHEAD (FDH), RESPONSIVE TO DESICCATION 26 (RD26), ARS-binding factor 2 (ABF2), WRKY75, and ferritin (FER). Overall, our work demonstrates the effects of rootstock on scion at the transcriptional level after drought stress and provides theoretical support for further understanding and utilization of *MdGH3* RNAi plants.

Keywords: transcriptome; apple; drought stress; GH3; grafting



Citation: He, J.; Guo, J.; Jiang, L.; An, W.; Ma, F.; Guan, Q.; Niu, C.

Transcriptional Effects of Rootstock on Scion after Drought: A Case Study of Using *MdGH3* RNAi as the Rootstock. *Horticulturae* **2022**, *8*, 1212. <https://doi.org/10.3390/horticulturae8121212>

Academic Editor: Hrotkó Károly

Received: 15 November 2022

Accepted: 15 December 2022

Published: 17 December 2022

Publisher's Note: MDPI stays neutral with regard to jurisdictional claims in published maps and institutional affiliations.



Copyright: © 2022 by the authors. Licensee MDPI, Basel, Switzerland. This article is an open access article distributed under the terms and conditions of the Creative Commons Attribution (CC BY) license (<https://creativecommons.org/licenses/by/4.0/>).

1. Introduction

Under natural conditions, plants are exposed to various environmental stresses such as drought, high salinity, and extreme temperatures during their growth and developmental stages [1]. Over the last few years, the crop yield and quality have suffered serious challenges with the frequency of climate changes [2]. Drought reduces photosynthetic rate by affecting stomatal status, leaf area, and metabolic rate changes through the accumulation of reactive oxygen species (ROS), thus reducing crop yield [3–6]. Drought occurs mainly in arid and semiarid regions, such as northwestern China, which is an important production area for high-quality apples [7]. Apple is one of the world's most popular fruits and is frequently threatened by drought [7]. Therefore, addressing the molecular mechanisms of apple production and fruit quality improvement under drought is of importance.

Perennial woody plants including apple have a long growth cycle; therefore, it is very challenging to breed varieties with drought tolerance using the traditional methods that select desirable traits from crossbreeding plants [8]. Therefore, design techniques have been developed to facilitate plant breeding efficiency, such as RNA interference (RNAi) and the clustered regularly interspaced short palindromic repeats (CRISPR)/CRISPR-associated (Cas) system [9–13]. For example, knocking out the *Mildew Locus O (MLO)* gene in grapevine could improve resistance to powdery mildew [14,15]. In citrus, the susceptible gene *LATERAL ORGAN BOUNDARIES 1 (CsLOB1)* promoter modified by CRISPR/Cas9 can improve resistance to canker [16]. In apple, resistance to fire blight disease could be enhanced by targeting *DspE-interacting proteins of Malus 1 (DIPM-1)*, *DIPM-2* and *DIPM-4* used with DNA-free genetic editing [14]. Knocking down six GRETCHEN HAGEN3 genes increases drought tolerance, water use efficiency, flowering, fruit setting, and fruit quality.

The GH3 family genes are involved in the conjugation of indole-3-acetic acid (IAA) [17,18], a process responsible for the balance of auxin [19]. *GH3* overexpression in rice reduces abscisic acid (ABA) levels and drought tolerance [20]. In cotton, reduced *GH3.5* expression levels increases plant tolerance to drought and salt stress [21]. In *Malus sieversii*, *GH3* genes are significantly induced by ABA [22]. Increased expression of *MsGH3.5* in M26 (an apple rootstock) results in a significant decrease in IAA content but an increase in cytokinin, leading to a dwarf phenotype with fewer adventitious roots [23]. *GH3.6*, another IAA conjugation enzyme, is a negative regulator of water deficit stress in apple. The transgenic apple plants knocking down *MdGH3.6* and its five homolog genes (*MdGH3 RNAi* transgenic plants) exhibit higher adventitious root number, longer roots, increased water use efficiency, and more cuticular wax under water-deficit stress [8].

Grafting, a traditional and commonly used method to fuse plant materials from two different plants, is widely applied in apple cultivation [7,24]. Grafting can improve abiotic and biotic resistance, accelerate flowering, shorten the juvenile period, and facilitate high-quality fruits [25,26]. Fuji (a popular commercial variety) grafted onto *MdGH3 RNAi* transgenic plants (Fuji/*MdGH3 RNAi*) show increased drought tolerance, water use efficiency, flowering, and fruit quality after drought, as compared with Fuji grafted onto the non-transgenic GL-3 plants (Fuji/GL-3) [8]. However, the molecular mechanisms behind this phenomenon remain unknown.

2. Materials and Methods

2.1. Plant Materials

The plant materials used in this study were generated previously [8,27]. Briefly, GL-3 (selected from progenies of *Malus × domestica* “Royal Gala”, and used as the non-transgenic control) and *MdGH3 RNAi* (knockdown of *MdGH3.6* and its five close paralogs) transgenic plants were the rootstocks, while *M. × domestica* “Fuji” plants were used as the scions, resulting in the grafted plants of “Fuji”/GL-3 or “Fuji”/*MdGH3 RNAi*.

28 grafted plants (14 plants for each group) were cultivated in a greenhouse located at the Northwest Agriculture and Forest University, Yangling (34°20' N, 108°24' E), Shaanxi Province, China. The average altitude of the greenhouse is 435 m, the average annual temperature inside the greenhouse is around 15 °C, and the plants grow under ambient light inside the greenhouse. All plants were transplanted into plastic pots (30 cm × 18 cm) filled with equal volumes of local loess sand and wormcast medium. Seven “Fuji”/GL-3 and seven “Fuji”/*MdGH3 RNAi* were subjected to a long-term drought treatment (60 days) as described previously in the first year of growth [27]. After that, the plants grew normally and were watered on average 3–5 times a week in summer and 1–2 times a week in winter, each time with 2 L of water. In addition, Hoagland’s nutrient solution was applied every 3–5 weeks according to the plant growth status [28]. On the third year of grafting, the fifth to ninth mature leaves (from top to bottom) from the scions and rootstocks were collected. All the above operations were completed in the same greenhouse.

2.2. RNA Extraction and Sequencing Procedures

Total RNAs were extracted with a cetyltrimethylammonium bromide (CTAB)-based method, as described previously [29]. The quality and concentration of RNA were checked with an Agilent Bioanalyzer 2100 system (Agilent Technologies, Santa Clara, CA, USA) and NanoDrop spectrophotometer (Thermo Scientific, Wilmington, DE, USA). RNA sequencing was performed using the Illumina HiSeq 4000 platform with paired-end, 150-base reads at Novogene (Beijing, China).

2.3. RNA-Seq Analysis

Raw data of RNA-seq were trimmed to remove adapters and low-quality bases (<20) using FastQC v0.11.9 and Trim Galore v0.6.6 (https://www.bioinformatics.babraham.ac.uk/projects/trim_galore/, accessed on 30 August 2022) in order to obtain clean reads [30]. The clean reads were aligned with the latest GDDH13 reference genome (v1.1, https://iris.angers.inra.fr/gddh13/downloads/GDDH13_1-1_formatted.fasta.bz2, accessed on 30 August 2022) using HISAT2 v4.8.2 [31–33]. Default parameters were used except for the following: {score algorithm `-score-min L,0,-0.2`}, `-pen-noncansplice 0`, `-max-intronlen 50000`, `-no-discordant`. Output files were filtered using SAMtools v1.9 and the parameter `"-bq 1"` was used to remove alignments with more than one valid alignment position [34]. Reads counting within genes region was obtained using GDDH13 gene annotation file (gff3 format file, https://iris.angers.inra.fr/gddh13/downloads/gene_models_20170612.gff3.bz2, accessed on 30 August 2022) by HTSeq v0.12.4 [33,35]. Differentially expressed genes were analyzed by R package DESeq2 v1.30.1 with thresholds of adjusted p value below 0.05 and the absolute value of log₂(fold change) greater than 1 [36]. Fragments per kilobase of transcript per million fragments mapped (FPKM) values were calculated by TBtools v1.09876 with effective gene length matrix obtained using R package GenomicFeatures v1.42.3 and the matrix for recording reads count modified from HTSeq results [37,38]. Heatmap plots were drawn using R package pheatmap v1.0.12. AgriGO v2.0, clusterProfiler v3.18.1 and ggplot2 v3.3.6 were used to complete Gene Ontology (GO) enrichment analyses [39–41]. Principal component analysis (PCA) analysis was performed using prcomp in R package stats v3.5.0. A Pearson correlation test was conducted using 'plotCorrelaation' tool in deepTools v3.5.1 [42].

2.4. Mobile mRNA Identification by RNA-Seq

RNA-seq data of the scion part all grafted plants were first mapped to the reference transcript sequence (https://iris.angers.inra.fr/gddh13/downloads/GDDH13_1-1_mrna.fasta.bz2, accessed on 30 August 2022) using "mem" in BWA v0.7.17-r1188 with default parameters [43]. In order to obtain the respective mate, the pair reads both maps concordantly to the same transcript, retention was performed according to SAM flags (83,163 or 99,147) and an insert size of 50 to 120 nt. BAM format file conversion, sorting, and indexing were performed using SAMtools [34]. Data variation was detected by the "mpileup" tool in SAMtools. Long-distance mRNA mobility was detected by SNPs substitution instead of indels and chromosomal rearrangements. Calling of sample alleles were carried out using VarScan v2.4.4, with parameters of minimum read depth at a position higher than 30 and minimum supporting reads at a position higher than 2 [44]. In addition, ambiguous bases ("N") in any dataset were excluded; only A, T, C, or G were left. Significant SNPs were required to exhibit exactly in two different alleles. For each sample, only SNPs appeared in two biological replicates were merged and retained using "isec" tools in BCFtools v1.8 [34]. Informative SNPs for the identification of mobile mRNAs moved from rootstock to scion were required to show homozygous alleles. Unique SNPs appearing only in Fuji/*MdGH3* RNAi scion data but not in Fuji/GL-3 scion data with control and drought treatment were used for further analysis. Overlapping SNPs between Fuji/*MdGH3* RNAi scion data and Fuji/GL-3 scion data under control and drought treatment were filtered. Furthermore, the overlapping mRNAs corresponding to the above SNPs in Fuji/*MdGH3* RNAi and Fuji/GL-3 under control and drought treatment were produced. Finally, mRNAs that

appeared only in the scion data of Fuji/*MdGH3* RNAi under control and drought were strictly considered as mRNAs moved from *MdGH3* RNAi rootstock to the Fuji scion.

3. Results

3.1. Phenotypic Comparison and Transcriptome of Grafted Plants Using *MdGH3* RNAi and GL-3 Plants as Rootstocks

Previously, we found that after long-term drought, *MdGH3* RNAi transgenic plants had higher plant height, stem diameter, dry weight of roots, dry weight of shoots, root-to-shoot ratio, photosynthetic rate, stomatal conductance, intercellular CO₂, transpiration rate, shoot hydraulic conductivity, root hydraulic conductivity, carbon isotope composition ($\delta^{13}\text{C}_{\text{PDB}}$), and intrinsic water use efficiency (WUEi), as compared to GL-3 [8]. We grafted the commercial apple variety “Fuji” onto *MdGH3* RNAi transgenic (Fuji/*MdGH3* RNAi) and GL-3 (Fuji/GL-3) plants, and performed a long-term drought treatment. Compared to Fuji/GL-3, the scions of drought-treated Fuji/*MdGH3* RNAi plants showed greater drought tolerance and higher flowering rate and fruit quality [8]. Under control conditions, compared to Fuji/GL-3, the scions of Fuji/*MdGH3* RNAi plants showed higher flowering rate, $\delta^{13}\text{C}_{\text{PDB}}$, soluble content, starch content, and C/N ratio, but lower total N content, and had fruits. Compared to Fuji/GL-3, the scions of drought-treated Fuji/*MdGH3* RNAi plants showed higher plant height, photosynthetic rate, stem diameter, $\delta^{13}\text{C}_{\text{PDB}}$, flowering rate, soluble content, starch content, C/N ratio, fruit diameter, fruit length, fruit weight, fruit pulp crispness, fruit firmness, fruit soluble solids content (SSC), fruit acidity, and sugar–acid ratio, and lower total N content. [8,27].

To understand the mechanisms behind the above phenomena, we carried out transcriptome sequencing (RNA-seq) of the scion and rootstock from Fuji/GL-3 (Figure 1a) and Fuji/*MdGH3* RNAi (Figure 1b) under control and drought treatment. Two biological replicates were prepared for each library. As shown in Table 1 after quality control, 18.70–24.54 million clean reads were generated for each sample. The mapping ratios were around 93.06–98.89. Pearson correlation coefficients between two biological replicates of samples showed reliable reproducibility (Figure 1). All these results suggested that the RNA-seq data could be used for further studies.

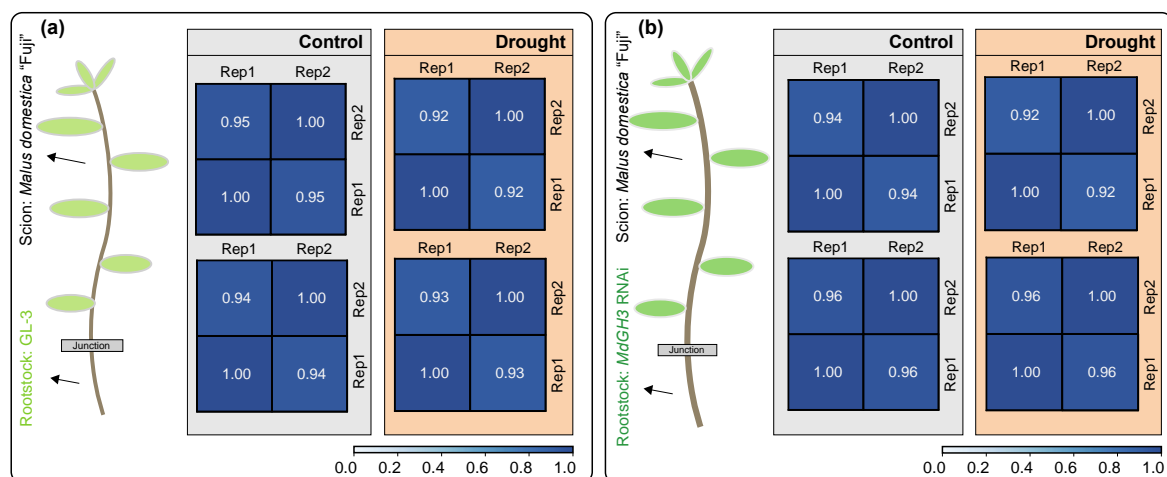


Figure 1. Experimental design of grafting and transcriptome sequencing. (a) *Malus domestica* “Fuji” (scion) were grafted onto GL-3 plants (rootstock) under control and drought conditions. (b) *Malus domestica* “Fuji” (scion) were grafted on *MdGH3* RNAi plants (rootstock) under control and drought conditions. The grey and orange areas show the transcriptome sequencing of the corresponding tissues in (a,b). The blue squares indicate the Pearson correlation of RNA-seq data. Two independent biological replicates per set were used for sequencing.

Table 1. The Statistics of transcriptome sequencing (RNA-seq) data.

Sample	Raw Reads	Clean Reads	Raw Base (G)	Clean Base (G)	Q20 (%)	Q30 (%)	GC Content (%)	Mapping Ratio (%)
Control "Fuji/GL-3" Rep1	25,143,068	23,973,149	7.54	7.19	98.28	94.71	47.32	93.36
Control "Fuji/GL-3" Rep2	25,752,761	24,541,277	7.73	7.36	98.25	94.61	47.34	93.24
Control "Fuji/GL-3" Rep1	22,824,047	21,670,561	6.85	6.5	98.31	94.75	47.45	93.47
Control "Fuji/GL-3" Rep2	20,255,453	19,353,326	6.08	5.81	98.31	94.78	47.41	93.56
Control "Fuji/MdGH3 RNAi" Rep1	23,568,295	22,345,147	7.07	6.7	98.21	94.53	47.22	93.06
Control "Fuji/MdGH3 RNAi" Rep2	23,744,639	22,762,112	7.12	6.83	98.31	94.73	46.8	93.77
Control "Fuji/MdGH3 RNAi" Rep1	20,469,321	19,537,242	6.14	5.86	98.25	94.6	47.24	93.96
Control "Fuji/MdGH3 RNAi" Rep2	22,951,961	21,696,492	6.89	6.51	98.34	94.76	47.19	94.06
Drought "Fuji/GL-3" Rep1	20,040,778	18,701,561	6.01	5.61	98.29	94.72	47.14	93.33
Drought "Fuji/GL-3" Rep2	21,133,554	20,108,894	6.34	6.03	98.37	94.86	47.25	93.38
Drought "Fuji/GL-3" Rep1	20,435,878	19,390,591	6.13	5.82	98.36	94.91	47.35	93.51
Drought "Fuji/GL-3" Rep2	22,430,471	21,593,803	6.73	6.48	98.34	94.81	47.22	93.84
Drought "Fuji/MdGH3 RNAi" Rep1	21,519,114	20,814,869	6.46	6.24	98.34	94.78	47.12	93.53
Drought "Fuji/MdGH3 RNAi" Rep2	21,640,685	20,732,825	6.49	6.22	98.23	94.52	47.02	93.09
Drought "Fuji/MdGH3 RNAi" Rep1	25,823,890	24,540,545	7.75	7.36	97.67	93.23	47.09	98.89
Drought "Fuji/MdGH3 RNAi" Rep2	21,009,641	20,148,636	6.3	6.04	98.28	94.69	47.05	93.2

The underlines marked in the sample column showed the issue part of the grafting plants.

3.2. Differentially Expressed Genes (DEGs) in Scion and Rootstock under Control Conditions

Under control conditions, compared to Fuji/GL-3, Fuji/MdGH3 RNAi plants exhibited better developmental phenotypes and higher $\delta^{13}\text{C}_{\text{PDB}}$, especially for the fruit traits. To understand the phenotypic changes at gene expression level in the scion and rootstock of Fuji/MdGH3 RNAi and Fuji/GL-3 plants under control conditions, we analyzed the DEGs. As shown in Figure 2a, principal component analysis (PCA) showed that the scion transcriptome data of Fuji/MdGH3 RNAi and Fuji/GL-3 were separated into two groups on the PCA1 axis. When the identification threshold for DEGs was $|\log_2(\text{fold change})| > 1$ and adjusted p -value was < 0.05 , 667 up-regulated genes and 176 down-regulated genes were found in the Fuji grafted onto MdGH3 transgenic plants, compared to those grafted onto GL-3 (Figure 2b). GO enrichment analysis showed that these DEGs could be divided into two categories: (1) development and growth: developmental process, fruit development, cell division, cell wall modification, cell wall organization or biogenesis, microtubule-based process, response to hormone, steroid biosynthetic process, polysaccharide biosynthetic process, lipid modification and biosynthetic process, aromatic compound biosynthetic process and biosynthetic and metabolic process of phenol-containing compound, phenylpropanoid, lignin, flavonoid, and xylan (Figure 2c); (2) stress: response to stimulus, response to abiotic

stimulus, response to temperature stimulus, response to endogenous stimulus, response to light stimulus, response to heat, response to water deprivation, response to water (Figure 2d).

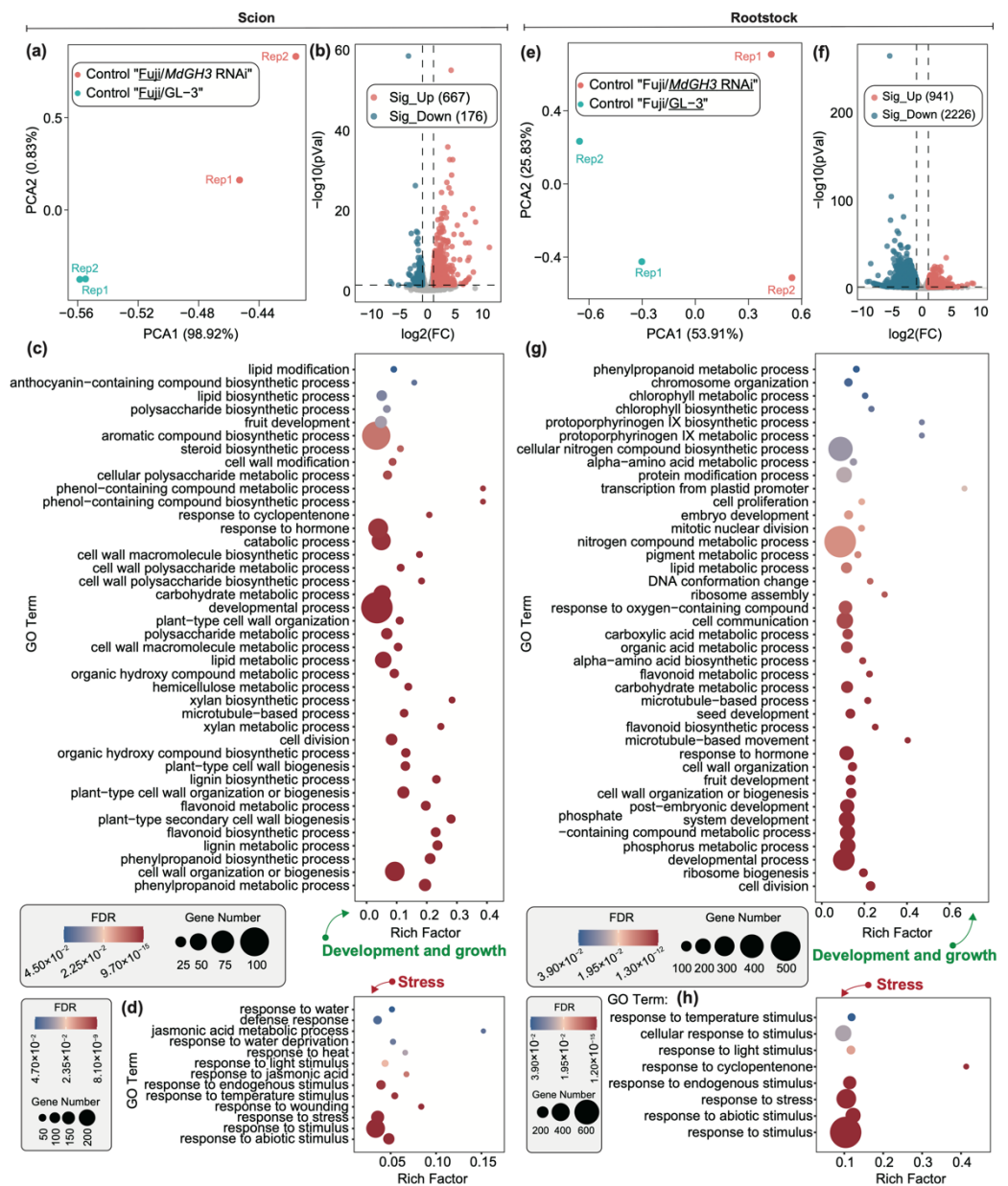


Figure 2. Differentially expressed genes (DEGs) in scion and rootstock of “Fuji/*MdGH3* RNAi” plants and “Fuji/GL-3” plants under control conditions. The left panel is the analysis of DEGs associated with scion, and the right one presents the DEGs associated with rootstock. (a) Principal component analysis (PCA) plot showing the variation between scion (“Fuji”) data of “Fuji/*MdGH3* RNAi” and “Fuji/GL-3”. (b) Volcano plot showing up-regulated genes and down-regulated genes in scion of “Fuji/*MdGH3* RNAi” compared to “Fuji/GL-3” under control conditions. (c,d) gene ontology (GO) enrichment analysis of DEGs in scion. (e) PCA plot showing the variation between rootstock of Fuji/*MdGH3* RNAi and Fuji/GL-3 data. (f) Volcano plot showing up- and down-regulated genes in *MdGH3* RNAi rootstocks compared to GL-3 rootstocks. (g,h) GO enrichment analysis of DEGs in rootstocks. The GO enrichment analysis in (c,d,g,h) was divided into “development and growth” and “stress” aspects.

We analyzed the DEGs of the rootstock in Fuji/*MdGH3* RNAi and Fuji/GL-3 plants using the same analytical methods. The PCA showed that the rootstock transcriptome data of Fuji/*MdGH3* RNAi and Fuji/GL-3 were also separated into two groups on the PCA1 axis (Figure 2e). The volcano plot showed that 941 genes were up-regulated and 2226 genes were down-regulated in *MdGH3* RNAi rootstock compared to GL-3 rootstock (Figure 2f). Similarly, GO enrichment analysis suggested that DEGs in rootstock of *MdGH3* RNAi and GL-3 were also enriched in two categories including “development and growth” and “stress”. Development and growth-related GO terms included: developmental process, system development, fruit development, seed development, embryo development, cell division, cell proliferation, cell communication, cell wall organization or biogenesis, microtubule-based movement, response to hormone, flavonoid biosynthetic and metabolic process, carbohydrate metabolic process, alpha-amino acid biosynthetic and metabolic process, lipid metabolic process, pigment metabolic process, nitrogen compound metabolic process, protoporphyrinogen IX biosynthetic and metabolic process, chlorophyll biosynthetic and metabolic process, and phenylpropanoid metabolic process (Figure 2g). GO terms regarding stress included: response to stimulus, response to abiotic stimulus, response to endogenous stimulus, response to light stimulus and response to temperature stimulus. These results suggested that changes of gene expression in rootstock of Fuji/*MdGH3* RNAi might be involved in metabolism and synthesis of growth substance, cell division, and proliferation to regulate development and basal drought tolerance.

To further understand which DEGs were involved in regulating the scion and rootstock biological processes of Fuji/*MdGH3* RNAi plants under control conditions, we selected some representative genes and performed heatmap plots (Figure 3). In Figure 3a–c, we displayed representative DEGs related to growth and stress response in scion of Fuji/*MdGH3* RNAi plants as compared to that of Fuji/GL-3. We found that two *FLAVONOL SYNTHASE 1 (FLS1)* genes were up-regulated in scion of Fuji/*MdGH3* RNAi plants. High expression of *FLS1* has been shown to positively correlate with strong flavanol accumulation in flowers, shoots, and at the junction of roots and shoots [45]. Two *heat shock protein 20s (HSP20s)* that can improve plant heat tolerance by preventing aggregation and irreversible denaturation of heat-denatured proteins were found to be upregulated in Fuji/*MdGH3* RNAi plants compared to Fuji/GL-3 [46]. In addition, two *HSP21s* and two *HSP70s* were also up-regulated. *HSP21* has been reported to promote carotenoid accumulation during tomato fruit ripening [47]. *HSP70* is essential for plants under normal growth and heat conditions [48]. We also found higher expression of six *laccases (LACs)*, six *Cellulose synthase A genes (CESAs)*, five *MYB DOMAIN PROTEINs (MYBs)*, three *WRKYs*, two *Dehydration-responsive-element-binding protein 1 genes (DREB1C)*, and two *ECERIFERUM 4 genes (CER4)* in scion of Fuji/*MdGH3* RNAi plants compared to Fuji/GL-3. *LAC4*, *LAC17*, and *LAC12* have been reported to play a positive role in the biosynthesis of lignin in *Arabidopsis thaliana* and cowpea. In poplar, transgenic plants with knockdown of *PtrCesA4*, *PtrCesA7* and *PtrCesA8* show a significant decrease in cellulose content, stunted growth, as well as early necrosis [49]. Down-regulation of *AtMYB103* during another development in *Arabidopsis* led to early tapetal degeneration and pollen aberration [50]. In *Arabidopsis*, the flavanol biosynthesis is transcriptionally controlled by *MYB12* and *MYB111*, and these two regulators can activate the biosynthetic enzymes encoding *FLS1* [51]. The *Arabidopsis MYB113*-overexpression plants show a large pigmentation increase [52]. Regarding *WRKY* transcription factors, the triple mutants of *WRKY25*, *WRKY26*, and *WRKY33* are more sensitive to heat stress compared to wild-type plants and show reduced germination, decreased survival, and increased electrolyte leakage [53]. In terms of *DREB1C*, the introduction of *DREB1C* has been reported to enhance drought tolerance in peanuts [54]. *MdCER4* has been reported to play an active role in apple fruit cuticular synthesis [55]. Additionally, flowering-associated *ANTHOCYANIN11 (ATAN11)* and *TSO1*, xylan- and pectin-associated *GALACTURONOSYLTRANSFERASE 12 (GAUT12)*, drought-related *sucrose vacuolar invertase (ATBETAFRUCT4)* and other development and growth positively

regulated genes (Figure 3a–c) were also up-regulated in scion of Fuji/*MdGH3* RNAi plants relative to Fuji/GL-3 plants [56–59].

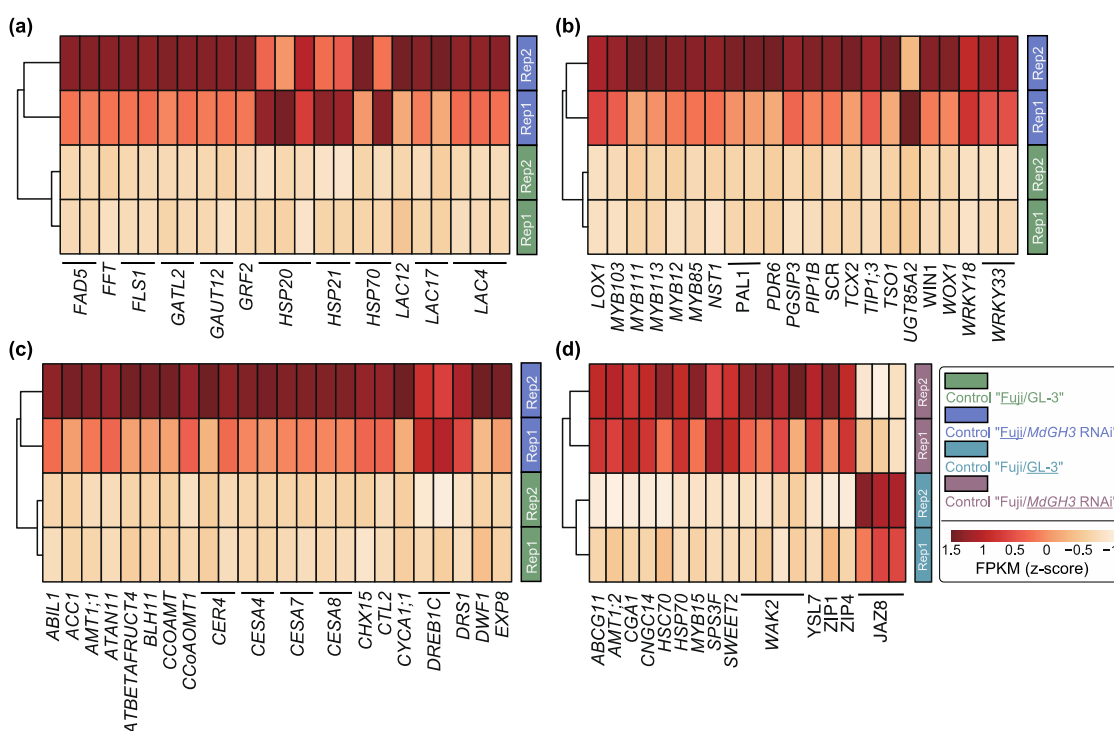


Figure 3. Heatmap plots show the differentially expressed genes (DEGs) associated with stress and growth in scion and rootstock obtained by comparing “Fuji/*MdGH3* RNAi” plants with “Fuji/GL-3” plants under control conditions. (a–c) DEGs in scion obtained by comparing “Fuji/*MdGH3* RNAi” to “Fuji/GL-3” under control conditions. (d) DEGs in rootstock obtained by comparing “Fuji/*MdGH3* RNAi” to “Fuji/GL-3” under control conditions.

Similarly, 16 up-regulated and 3 down-regulated genes in the rootstock part of Fuji/*MdGH3* RNAi plants were exhibited as compared to “Fuji”/GL-3 (Figure 3d). The up-regulated genes included: *wall-associated kinase 2* (WAK2), *ARABIDOPSIS THALIANA WHITE-BROWN COMPLEX HOMOLOG PROTEIN 11* (ABCG11), *Ammonium transporter 1 member 1* (AMT1), *CYTOKININ-RESPONSIVE GATA FACTOR 1* (CGA1), *cyclic nucleotide-gated channel 14* (CNGC14), *Heat Shock Cognate Protein 70* (HSC70), *HSP70*, *MYB15*, *SUCROSE PHOSPHATE SYNTHASE 3F* (SPS3F), *SWEET2*, *YELLOW STRIPE LIKE 7* (YSL7), *ZINC TRANSPORTER 1 PRECURSOR* (ZIP1), and *ZIP4*. WAK2 can actively promote cell expansion in *Arabidopsis* [60]. *Arabidopsis ABCG11* has been shown to be required for various cuticular lipids synthesis [61]. Reconstitution of *AMT1;3* expression in *amt1;3-1 Arabidopsis* mutant plants has restored higher-order lateral root development [62]. *CGA1* plays an important role in chloroplast development, growth, and division in *Arabidopsis* [63]. Down-regulation of *CNGC14* expression in *Arabidopsis* leads to shorter root hairs [64]. *SPS3F* is associated with starch, sucrose and energy metabolism [65]. In *Medicago truncatula*, *MtYSL7* mutant plants exhibit reduced nitrogen fixation and plant growth [66]. In maize and poplar, *ZIP1* and *ZIP4* mediate the development of lateral root and drought tolerance [67,68]. Three down-regulated genes in rootstock of Fuji/*MdGH3* RNAi relative to GL-3 were *JASMONATE ZIM-DOMAIN 8* (*JAZ8*). It has been reported that the accumulation of *JAZ8* in *Arabidopsis* lead to a reduction in root hair length [69]. Therefore, the above results show that the transcript levels of numerous genes were greatly increased in scion and rootstock of Fuji/*MdGH3* RNAi transgenic plants under control conditions, as compared to GL-3. These genes were related to reproductive organ development and maturation,

growth and stress response, which might contribute to the phenotypes of Fuji/*MdGH3* RNAi transgenic plants.

3.3. DEGs in Drought-Treated Scion and Rootstock

Drought tolerance is an important characteristic of *MdGH3* RNAi transgenic plants, and drought-treated “Fuji” grafted onto *MdGH3* RNAi plants possessed better drought tolerance as well as fruit quality compared to ‘Fuji’ grafted onto GL-3. Therefore, we used RNA-seq to investigate the molecular differences between Fuji/*MdGH3* RNAi and Fuji/GL-3 plants after drought at the transcriptional level.

As shown in Figure 4a, PCA results showed that RNA-seq data of drought-treated scion from Fuji/*MdGH3* RNAi and Fuji/GL-3 were divided into two parts. A small number of DEGs were identified, including 17 up-regulated and 15 down-regulated genes in drought-treated scion of Fuji/*MdGH3* RNAi compared to that of Fuji/GL-3 (Figure 4b). GO enrichment analysis of these 32 DEGs generated a total of six significant GO terms, including response to stimulus, carbohydrate metabolic process, organic substance metabolic process, single-organism process, metabolic process, and primary metabolic process. Compared to drought-treated scion comparisons, rootstock comparisons between Fuji/*MdGH3* RNAi and Fuji/GL-3 after drought showed dramatic transcript changes. PCA showed that RNA-seq data of drought-treated rootstock in Fuji/*MdGH3* RNAi and Fuji/GL-3 was divided into two groups, indicating that data can be used for further comparison (Figure 4d). The volcano plot showed that 220 up-regulated and 452 down-regulated genes were identified in the drought-treated rootstock of Fuji/*MdGH3* RNAi compared to the drought-treated rootstock of Fuji/GL-3 (Figure 4e). We performed GO enrichment analysis of these DEGs and found the significant GO terms related to stress included: response to abiotic stimulus, response to nutrient levels, response to extracellular stimulus, response to starvation, and response to endogenous stimulus (Figure 4f). The significant GO terms related to development and growth included: cell division, microtubule-based process and movement, response to hormone, lignin metabolic process and metabolic and biosynthetic process of organonitrogen compound, peptide, flavonoid, pigment, and nitrogen compound (Figure 4g). These data implied that *MdGH3* RNAi rootstock may facilitate drought stress tolerance of scion through promoted scion growth and stress response.

Despite the low number of DEGs identified in the scion fraction, we still found up-regulated *Aminopeptidase M1 (APM1)* and down-regulated *Senescence-associated carboxylesterase 101 (SAG101)*. In *Arabidopsis*, *APM1* loss-of-function mutants cause seedling death [70]. The decreased expression levels of *SAG101* and *SAG102* in exogenous PopW treatment may be important in delaying senescence in alfalfa due to drought stress [71]. The whole genes in Figure 5 were derived from the up-regulated DEGs database from the rootstock part of drought-treated “Fuji”/*MdGH3* RNAi compared to “Fuji”/GL-3. As shown in Figure 5, these genes included *AMT2*, *ATB2s*, *Cu/Zn superoxide dismutase 1 (CSD1)*, *DIHYDROFLAVONOL-4-REDUCTASE (DFR)*, *ferritin 1 genes (FER1s)*, *FASCICLIN-like arabinogalactan-protein 11 (FLA11)*, *FLA12*, *3-KETOACYL-COA SYNTHASE 19 (KCS19)*, *LAC12*, *LAC4*, *SPS3F*, *HOPW1-1-INTERACTING 1 (WIN1)*, *WRKY57*, *WRKY6*, and *YSL7*. In *Arabidopsis*, *ATB2* expression increased under low osmotic conditions [72]. Transgenic *Arabidopsis* plants expressing *AhCSD1* were more tolerant to osmotic stress [73]. Up-regulated genes *FLA11* and *FLA12* involved in leaf cuticle and wax could improve tolerance to water loss in ryegrass and poplar [74,75]. More wax was accumulated in the leaves of *WIN1*-overexpressing *Arabidopsis* transgenic plants [76]. Therefore, these transcriptional changes may contribute to the better growth and fruit quality of Fuji/*MdGH3* RNAi compared to Fuji/GL-3 after drought treatment.

3.4. Identification of Mobile mRNAs Moving from *MdGH3* RNAi Rootstock to Scion

It has been reported that mobile mRNAs (mb-mRNAs) have an effect on the development of their destination tissues. Some mRNAs encoding transcribed non-cell-autonomous proteins move through the plasmodesmata (PD) and post-translationally regulate meris-

tematic tissue development, leaf shape, fruit size, tuberization, and root structure [77–81]. Thus, identification of mb-mRNAs that moved from *MdGH3* RNAi rootstock to scion was important to fully understand the superior phenotypes of Fuji/*MdGH3* RNAi plants under control and drought treatment. In Figure 6a, the overall presence of substitution SNPs in scion of Fuji/*MdGH3* RNAi and Fuji/GL-3 under control and drought were inspected. Under control conditions, 2556 and 2260 SNPs were found in the scion of Fuji/GL-3 and Fuji/*MdGH3* RNAi, respectively. Meanwhile, 2674 and 2100 SNPs were found in the scion of drought-treated Fuji/GL-3 and Fuji/*MdGH3* RNAi, respectively. By removing common SNPs and mb-mRNAs between scion of Fuji/GL-3 and Fuji/*MdGH3* RNAi under control and drought treatment, 365 and 300 mb-mRNAs were found to potentially move from *MdGH3* RNAi rootstock to the scion under control and drought, respectively (Figure 6a).

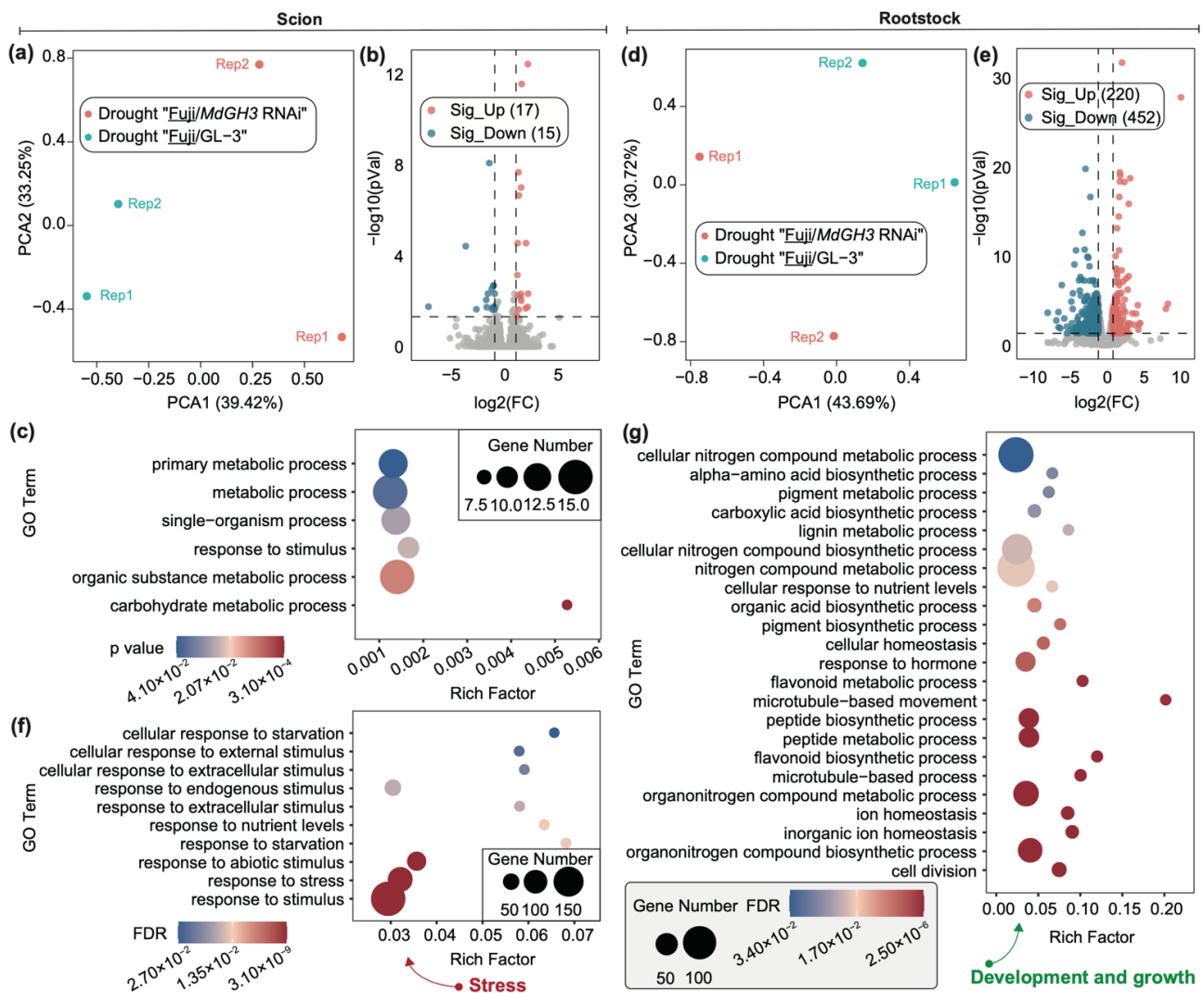


Figure 4. Differentially expressed genes (DEGs) in scion and rootstock obtained by comparing drought-treated “Fuji/*MdGH3* RNAi” plants with drought-treated “Fuji/GL-3” plants. (a) PCA plot showing the variation between scion (‘Fuji’) data of drought-treated “Fuji/*MdGH3* RNAi” and drought-treated “Fuji/GL-3”. (b) Volcano plot showing up- and down-regulated genes in scion of “Fuji/*MdGH3* RNAi” compared to “Fuji/GL-3” under drought conditions. (c) GO enrichment analysis of DEGs in scion. (d) PCA plot showing the variation between drought-treated rootstock (*MdGH3* RNAi and GL-3) data of “Fuji/*MdGH3* RNAi” and “Fuji/GL-3”. (e) Volcano plot showing up- and down-regulated genes in drought-treated *MdGH3* RNAi plants compared to drought-treated GL-3. (f, g) GO enrichment analysis of DEGs in rootstock. The GO terms were divided into “development and growth” and “stress” aspects.

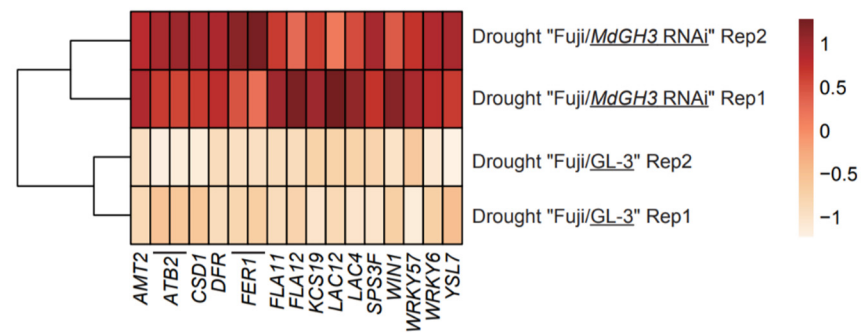


Figure 5. Heatmap of expression levels (in the form of z-score fragments per kilobase of transcript per million fragments mapped) showing the stress and growth-related DEGs in rootstock obtained by comparing drought-treated “Fuji/*MdGH3* RNAi” plants to drought-treated “Fuji/*GL-3*” plants.

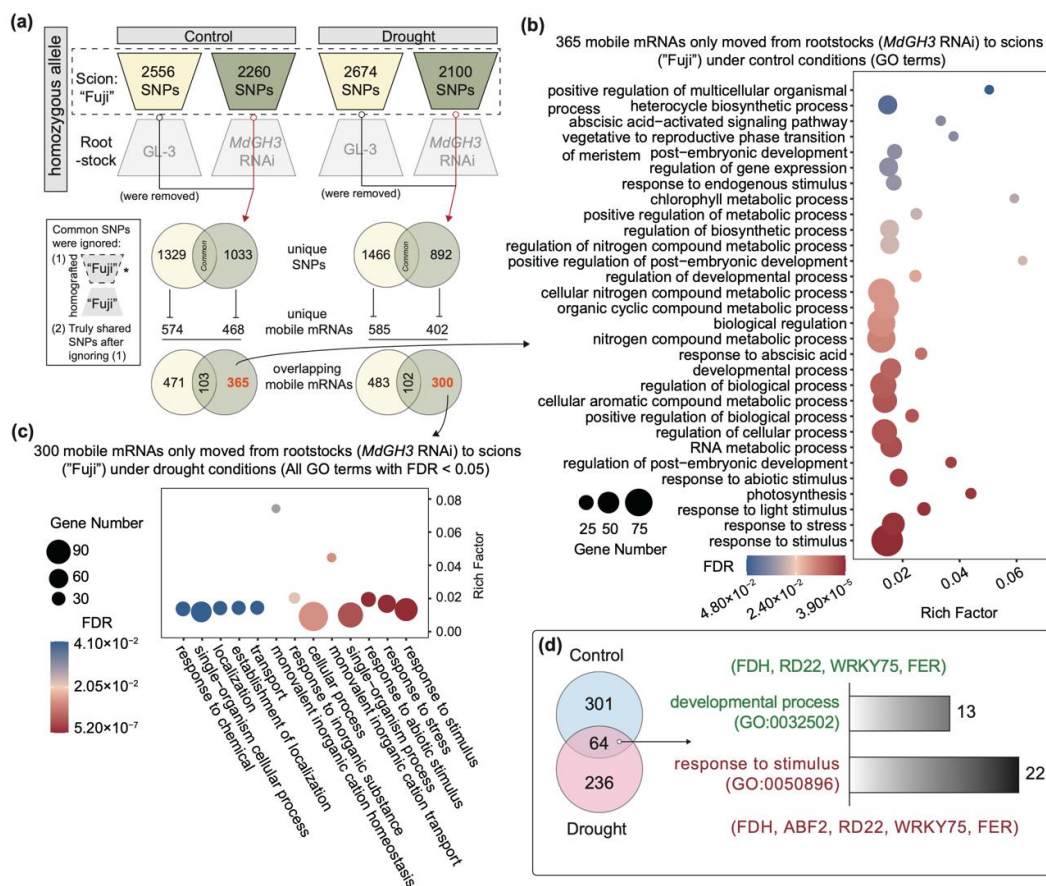


Figure 6. Detection of mRNA movement from control and drought-treated *MdGH3* RNAi rootstock to scion (“Fuji”). (a) Movement of mRNAs from control and drought-treated *MdGH3* RNAi rootstock to the scion. The pipeline included variant calling and mobile mRNAs detection. Green circles and trapezoidal patterns represent SNPs data and mobile mRNAs (mb-mRNAs) moving from rootstocks *MdGH3* RNAi plants to scion. The yellow circles and trapezoidal patterns represent SNPs data and mobile mRNAs moving from rootstock *GL-3* to scion. (b) GO enrichment analysis of 365 mb-mRNAs moving from *MdGH3* RNAi rootstock to scion under control conditions. (c) GO terms of 300 mb-mRNAs moving from drought-treated *MdGH3* RNAi plants rootstock to drought-treated scion. (d) Venn diagram demonstrating that 64 mb-mRNAs moved from *MdGH3* RNAi plants to scion under control as well as drought treatment. Barplot showing the two GO terms including “developmental process (GO:0032502)” and “response to stimulus (GO:0050896)”, and the number of mb-mRNAs in them. Green font was used for mb-mRNAs related to “developmental process (GO:0032502)”, and red font was used for those related to “response to stimulus (GO:0050896)”.

GO enrichment analysis of 365 and 300 mb-mRNAs were performed to determine their functional classification. For the 365 mb-mRNAs that only moved from *MdGH3* RNAi rootstock to scion under control conditions, significant GO classification mainly included: (1) stress: response to abiotic stimulus, response to abscisic acid, abscisic acid-activated signaling pathway, response to light stimulus, and response to endogenous stimulus; (2) development and growth: development process, positive regulation of biological process, photosynthesis, regulation of post-embryonic development, cellular aromatic compound metabolic process, nitrogen compound metabolic process, chlorophyll metabolic process, post-embryonic development, vegetative to reproductive phase transition of meristem, and heterocycle biosynthetic process (Figure 6b). The significant GO terms of 300 mb-mRNAs that only moved from drought-treated *MdGH3* RNAi rootstock to scion mainly contained response to stimulus, response to abiotic stimulus, response to stress, transport, and establishment of localization (Figure 6c). In addition, the Venn diagram in Figure 6 shows that among the 665 mb-mRNAs moving from *MdGH3* RNAi rootstock to scion, 301 moved only under control, 236 moved only after drought treatment, and 64 could move both under control and drought treatment. Further studies revealed that 13 mb-mRNAs were enriched to “developmental process (GO:0032502)” and 22 mb-mRNAs were enriched to “response to stimulus (GO:0050896)”. FIDDLEHEAD (FDH), RESPONSIVE TO DESICCATION 26 (RD26), WRKY75, and FER were found to be present in both pathways. ARS-binding factor 2 (ABF2) was found to occur only in “response to stimulus” (Figure 6D). The *fdh* mutation has deleterious effects on various aspects of cuticle quality, plant morphology, and trichome differentiation [82]. It has been reported that RD26 and its homologs function to promote the expression of drought-responsive genes and improve the drought tolerance of plants [83]. In *Arabidopsis*, *fer* mutant plants exhibited growth retardation and salt hypersensitivity [84]. *ABF2* has been reported to be required for normal glucose response and overexpression of *ABF2* enhanced *Arabidopsis* salt and drought tolerance [85]. These results suggested that, compared with Fuji/GL-3, mb-mRNAs which specifically moved from *MdGH3* RNAi rootstock to Fuji scion not only regulated growth and development but also conferred drought tolerance in the scion.

4. Discussion

The flexibility and integrity of cell structures and components are essential for plant growth and development [86–89]. In plant cells, microtubules (MTs) play an important role in cell division, expansion, and morphogenesis [89]. Rapid cell division and expansion during the early stages of fruit development is a requirement for yield and quality [90,91]. In cucumber, kinesin genes were identified from fruits of different sizes. Among these genes, *CsKF2-CsKF6* were associated with rapid cell production, and *CsKF1* and *CsKF7* were strongly positively correlated with rapid cell expansion [92]. MTs has also been reported to play a key role in the fine transport and repositioning of vesicles to maintain pollen tube growth [93]. The cell wall is also crucial for many processes of plant development, such as acting as a barrier to protect plants from environmental stress [87]. In addition, the biosynthesis and modification of cell wall polysaccharides have also been reported to largely contribute to fruit texture formation in apple [86]. In our GO enrichment analysis of DEGs in scion and rootstock of Fuji/*MdGH3* RNAi plants compared to ‘Fuji’/GL3 under control conditions, we identified relevant GO terms, including: cell division, cell wall organization or biogenesis, cell wall modification, and microtubule-based process. In the GO enrichment analysis of DEGs from rootstock of drought-treated Fuji/*MdGH3* RNAi relative to Fuji/GL-3 plants, we identified significant GO terms with cell division, microtubule-based process, and movement. These results suggest that MTs and cell walls may play an important role in grafted plants when *MdGH3* RNAi was used as rootstock.

Many substances have been involved in the biological processes of flowering, fruit development, and stress response [94–98]. Phenolic compounds exert antioxidant effects by reacting with various free radicals. The mechanism of action of antioxidants involves hydrogen atom transfer, transfer of a single electron, sequential proton loss electron transfer,

and chelation of transition metals [99]. Phenolic compounds derived from the phenylpropanoid pathway include anthocyanins, phenolic acids, flavonols, dihydrochalcone, and flavanols [100]. All these phenolic compounds are considered to be major contributors to the internal and external quality of apple fruit. Additionally, these compounds can also affect fruit resistance to *Botrytis cinerea* [101]. Polyphenols in apple fruits have been reported to improve human health as an indicator of fruit quality [102]. Anthocyanins are important flavonoid pigments that can protect pears from damage caused by high temperatures under high light [103]. Light can influence the production of secondary metabolites, such as lignin, which regulates apple fruit hardness and eating quality [104]. Lignin is a major component of the plant secondary cell wall and helps plants to resist various abiotic and biotic stresses. Notably, there is substrate competition between the biosynthesis of lignans and anthocyanins [104]. Brassinosteroids (BRs), a class of plant-specific steroidal phytohormones, have been reported to play multifunctional roles in developmental processes, including root/shoot growth, flowering, seed germination, senescence, and environmental stresses [105,106]. In our results, we found GO terms obtained from DEGs in scion of 'Fuji'/*MdGH3* RNAi compared to 'Fuji'/GL-3 under control conditions were related to steroid biosynthetic process, polysaccharide biosynthetic process, lipid modification, and biosynthetic process, aromatic compound biosynthetic process, and biosynthetic and metabolic processes of the phenol-containing compounds phenylpropanoid, lignin, flavonoid, and xylan. Similar results were obtained in the GO enrichment analysis of rootstock comparison between "Fuji"/*MdGH3* RNAi and "Fuji"/GL-3 plants. Similarly, drought-treated Fuji/*MdGH3* RNAi showed enriched GO terms including metabolic and biosynthetic process of flavonoid, pigment, and lignin in the rootstock part, compared to rootstock of Fuji/GL-3. These data indicate that the phenotypic changes using *MdGH3* RNAi transgenic plant as rootstock compared to GL-3 as rootstock may be attributed to changes in the levels of metabolites, such as phenylpropanoid, flavonoid, pigment, and lignin. However, further studies and measurements are needed including determining the changes of metabolite levels under control and after drought treatments in the grafted plants.

In higher plants, mRNA is mobile between the rootstock and the scion [25,107]. For example, *GAI* (Gibberellic acid insensitive) mRNA can move from rootstock to scion in *Malus* and *Pyrus* [108,109]. Further research demonstrated that *GAI* remains at the sites to which it is transported and causes the attenuation of GA responses [110]. An NAC domain protein that is involved in apical meristem development has been reported to move from rootstock to scion in grafted pears [111]. In the mobile mRNA dataset from *MdGH3* RNAi rootstock to scion, 301 moved only under control, 236 moved only after drought treatment, and 64 could move under both control and drought treatment. Furthermore, we identified mobile mRNAs which might be associated with stress and growth, such as homologs of *FDH*, *RD26*, *WRKY75*, *FER*, and *ABF2*. Under control conditions, only *RD26* was found to move from *MdGH3* RNAi rootstock to the scion and was up-regulated in the scion. However, the expression of *FDH*, *ABF2*, *WRKY75*, and *FER* were not found to be up-regulated in the scion. In previous studies, researchers have found that mRNA is degraded during movement and that mRNA expression levels are not good indicators for identifying movement [112]. Therefore, the movement of long-distance mRNAs remains complex and unknown. Taken together, further systematic validation of these mobile mRNAs in control and drought-treated grafted plants using *MdGH3* RNAi as rootstock is needed.

In summary, we performed and compared transcriptome sequencing of all scions and rootstocks of control and drought-treated grafted plants using *MdGH3* RNAi and GL-3 as rootstocks. Under control conditions, a large number of DEGs related to growth and development and resistance were identified in scions and rootstocks of grafted plants using *MdGH3* RNAi as rootstock and their functional enrichment was performed compared to grafted plants with GL-3 as rootstock. Under drought conditions, a few numbers of DEGs were obtained from the comparison of scion, but a large number of DEGs were still

found in the rootstock part of the grafted plants using *MdGH3* RNAi as rootstock and their functional analysis was also conducted. Moreover, we identified mRNAs that only moved from the *MdGH3* RNAi rootstock to scion. Mobile mRNAs moved in both control and drought conditions, including *FDH*, *ABF2*, *RD26*, *WRKY75*, and *FER*, which were associated with drought response and plant development. Our work provides the transcriptional explanation behind the phenotypic changes of *MdGH3* RNAi transgenic plants as rootstocks in field applications and data sources for genetic engineering to improved agricultural production.

Author Contributions: C.N., F.M., Q.G. and J.H. designed the study. L.J. prepared the plants. J.H., J.G. and W.A. analyzed the data. C.N., F.M., J.H. and Q.G. wrote the manuscript. All authors have read and agreed to the published version of the manuscript.

Funding: This research was supported by the National Key Research and Development Program of China (2019YFD 1000100) and the National Natural Science Foundation of China (31872080).

Institutional Review Board Statement: Not applicable.

Informed Consent Statement: Not applicable.

Data Availability Statement: The RNA-seq data have been deposited with the NCBI with the dataset identifier PRJNA901677.

Acknowledgments: We thank the High-Performance Computing (HPC) platform of Northwest A&F University (NWAUFU) for providing computing resources. We also thank Novogene (<https://www.novogene.com/>), accessed on 30 August 2022) for assistance with the RNA-seq assay.

Conflicts of Interest: The authors declare no conflict of interest.

References

1. Zhao, M.; Running, S.W. Drought-Induced Reduction in Global Terrestrial Net Primary Production from 2000 through 2009. *Science* **2010**, *329*, 940–943. [CrossRef] [PubMed]
2. Mao, X.; Hou, N.; Liu, Z.; He, J. Profiling of N6-Methyladenosine (M6A) Modification Landscape in Response to Drought Stress in Apple (*Malus Prunifolia* (Willd.) Borkh). *Plants* **2021**, *11*, 103. [CrossRef] [PubMed]
3. Tikkanen, M.; Grieco, M.; Aro, E.-M. Novel Insights into Plant Light-Harvesting Complex II Phosphorylation and ‘State Transitions’. *Trends Plant Sci.* **2011**, *16*, 126–131. [CrossRef]
4. Nishiyama, Y.; Allakhverdiev, S.I.; Murata, N. Protein Synthesis Is the Primary Target of Reactive Oxygen Species in the Photoinhibition of Photosystem II. *Physiol. Plant.* **2011**, *142*, 35–46. [CrossRef]
5. Gururani, M.A.; Venkatesh, J.; Tran, L.S.P. Regulation of Photosynthesis during Abiotic Stress-Induced Photoinhibition. *Mol. Plant* **2015**, *8*, 1304–1320. [CrossRef] [PubMed]
6. Foyer, C.H.; Shigeoka, S. Understanding Oxidative Stress and Antioxidant Functions to Enhance Photosynthesis. *Plant Physiol.* **2011**, *155*, 93–100. [CrossRef] [PubMed]
7. Li, Z.; Wang, L.; He, J.; Li, X.; Hou, N.; Guo, J.; Niu, C.; Li, C.; Liu, S.; Xu, J.; et al. Chromosome-scale Reference Genome Provides Insights into the Genetic Origin and Grafting-mediated Stress Tolerance of *Malus Prunifolia*. *Plant Biotechnol. J.* **2022**, *20*, 1015–1017. [CrossRef]
8. Jiang, L.; Shen, W.; Liu, C.; Tahir, M.M.; Li, X.; Zhou, S.; Ma, F.; Guan, Q. Engineering Drought-Tolerant Apple by Knocking down Six *GH3* Genes and Potential Application of Transgenic Apple as a Rootstock. *Hortic. Res.* **2022**, *9*, uhac122. [CrossRef]
9. Tzfira, T. Agrobacterium T-DNA Integration: Molecules and Models. *Trends Genet.* **2004**, *20*, 375–383. [CrossRef]
10. Terns, R.M.; Terns, M.P. CRISPR-Based Technologies: Prokaryotic Defense Weapons Repurposed. *Trends Genet.* **2014**, *30*, 111–118. [CrossRef]
11. Manghwar, H.; Lindsey, K.; Zhang, X.; Jin, S. CRISPR/Cas System: Recent Advances and Future Prospects for Genome Editing. *Trends Plant Sci.* **2019**, *24*, 1102–1125. [CrossRef] [PubMed]
12. Vuong, U.T.; Iswanto, A.B.B.; Nguyen, Q.; Kang, H.; Lee, J.; Moon, J.; Kim, S.H. Engineering Plant Immune Circuit: Walking to the Bright Future with a Novel Toolbox. *Plant Biotechnol. J.* **2022**, pbi.13916. [CrossRef] [PubMed]
13. Khawar, K.M.; Onarici, S.; Ozel, C.A.; Aasim, M.; Bakhsh, A.; Rao, A.Q. Plant Biotechnology. *Sci. World J.* **2013**, *2013*, 736731. [CrossRef] [PubMed]
14. Malnoy, M.; Viola, R.; Jung, M.-H.; Koo, O.-J.; Kim, S.; Kim, J.-S.; Velasco, R.; Nagamangala Kanchiswamy, C. DNA-Free Genetically Edited Grapevine and Apple Protoplast Using CRISPR/Cas9 Ribonucleoproteins. *Front. Plant Sci.* **2016**, *7*, 1904. [CrossRef]
15. Pessina, S.; Lenzi, L.; Perazzolli, M.; Campa, M.; Dalla Costa, L.; Urso, S.; Valè, G.; Salamini, F.; Velasco, R.; Malnoy, M. Knockdown of MLO Genes Reduces Susceptibility to Powdery Mildew in Grapevine. *Hortic. Res.* **2016**, *3*, 16016. [CrossRef]

16. Peng, A.; Chen, S.; Lei, T.; Xu, L.; He, Y.; Wu, L.; Yao, L.; Zou, X. Engineering Canker-Resistant Plants through CRISPR/Cas9-Targeted Editing of the Susceptibility Gene *CsLOB1* Promoter in Citrus. *Plant Biotechnol. J.* **2017**, *15*, 1509–1519. [[CrossRef](#)]
17. Östin, A.; Kowalczyk, M.; Bhalerao, R.P.; Sandberg, G. Metabolism of Indole-3-Acetic Acid in Arabidopsis1. *Plant Physiol.* **1998**, *118*, 285–296. [[CrossRef](#)]
18. Kowalczyk, M.; Sandberg, G. Quantitative Analysis of Indole-3-Acetic Acid Metabolites in Arabidopsis. *Plant Physiol.* **2001**, *127*, 1845–1853. [[CrossRef](#)]
19. Brunoni, F.; Collani, S.; Casanova-Sáez, R.; Šimura, J.; Karady, M.; Schmid, M.; Ljung, K.; Bellini, C. Conifers Exhibit a Characteristic Inactivation of Auxin to Maintain Tissue Homeostasis. *New Phytol.* **2020**, *226*, 1753–1765. [[CrossRef](#)]
20. Du, H.; Wu, N.; Fu, J.; Wang, S.; Li, X.; Xiao, J.; Xiong, L. A GH3 family member, OsGH3-2, modulates auxin and abscisic acid levels and differentially affects drought and cold tolerance in rice. *J. Exp. Bot.* **2012**, *63*, 6467–6480. [[CrossRef](#)]
21. Kirungu, J.N.; Magwanga, R.O.; Lu, P.; Cai, X.; Zhou, Z.; Wang, X.; Peng, R.; Wang, K.; Liu, F. Functional Characterization of Gh_A08G1120 (GH3.5) Gene Reveal Their Significant Role in Enhancing Drought and Salt Stress Tolerance in Cotton. *BMC Genet* **2019**, *20*, 62. [[CrossRef](#)]
22. Yuan, H.; Zhao, K.; Lei, H.; Shen, X.; Liu, Y.; Liao, X.; Li, T. Genome-Wide Analysis of the GH3 Family in Apple (*Malus × Domestica*). *BMC Genom.* **2013**, *14*, 297. [[CrossRef](#)] [[PubMed](#)]
23. Zhao, D.; Wang, Y.; Feng, C.; Wei, Y.; Peng, X.; Guo, X.; Guo, X.; Zhai, Z.; Li, J.; Shen, X.; et al. Overexpression of MsGH3.5 Inhibits Shoot and Root Development through the Auxin and Cytokinin Pathways in Apple Plants. *Plant J.* **2020**, *103*, 166–183. [[CrossRef](#)]
24. Harada, T. Grafting and RNA Transport via Phloem Tissue in Horticultural Plants. *Sci. Hortic.* **2010**, *125*, 545–550. [[CrossRef](#)]
25. Kehr, J.; Kragler, F. Long Distance RNA Movement. *New Phytol.* **2018**, *218*, 29–40. [[CrossRef](#)] [[PubMed](#)]
26. Westwood, J.H. RNA Transport: Delivering the Message. *Nat. Plants* **2015**, *1*, 15038. [[CrossRef](#)]
27. Jiang, L.; Zhang, D.; Liu, C.; Shen, W.; He, J.; Yue, Q.; Niu, C.; Yang, F.; Li, X.; Shen, X.; et al. MdGH3.6 Is Targeted by MdMYB94 and Plays a Negative Role in Apple Water-deficit Stress Tolerance. *Plant J.* **2022**, *109*, 1271–1289. [[CrossRef](#)]
28. Zhang, D.; Yang, K.; Kan, Z.; Dang, H.; Feng, S.; Yang, Y.; Li, L.; Nou, H.; Xu, L.; Wang, X.; et al. The regulatory module MdbT2–MdMYB88/MdMYB124–MdNRTs regulates nitrogen usage in apple. *Plant Physiol.* **2021**, *185*, 1924–1942. [[CrossRef](#)]
29. Chang, S.; Puryear, J.; Cairney, J. A Simple and Efficient Method for Isolating RNA from Pine Trees. *Plant Mol. Biol. Rep.* **1993**, *11*, 113–116. [[CrossRef](#)]
30. Fiancette, R.; Finlay, C.M.; Willis, C.; Bevington, S.L.; Soley, J.; Ng, S.T.H.; Baker, S.M.; Andrews, S.; Hepworth, M.R.; Withers, D.R. Reciprocal Transcription Factor Networks Govern Tissue-Resident ILC3 Subset Function and Identity. *Nat. Immunol.* **2021**, *22*, 1245–1255. [[CrossRef](#)]
31. Kim, D.; Langmead, B.; Salzberg, S.L. HISAT: A Fast Spliced Aligner with Low Memory Requirements. *Nat. Methods* **2015**, *12*, 357–360. [[CrossRef](#)] [[PubMed](#)]
32. Perteza, M.; Kim, D.; Perteza, G.M.; Leek, J.T.; Salzberg, S.L. Transcript-Level Expression Analysis of RNA-Seq Experiments with HISAT, StringTie and Ballgown. *Nat. Protoc.* **2016**, *11*, 1650–1667. [[CrossRef](#)] [[PubMed](#)]
33. Daccord, N.; Celton, J.-M.; Linsmith, G.; Becker, C.; Choisne, N.; Schijlen, E.; Van de Geest, H.; Bianco, L.; Micheletti, D.; Velasco, R.; et al. High-Quality de Novo Assembly of the Apple Genome and Methylome Dynamics of Early Fruit Development. *Nat. Genet.* **2017**, *49*, 1099–1106. [[CrossRef](#)]
34. Danecek, P.; Bonfield, J.K.; Liddle, J.; Marshall, J.; Ohan, V.; Pollard, M.O.; Whitwham, A.; Keane, T.; McCarthy, S.A.; Davies, R.M.; et al. Twelve Years of SAMtools and BCFtools. *GigaScience* **2021**, *10*, giab008. [[CrossRef](#)] [[PubMed](#)]
35. Anders, S.; Pyl, P.T.; Huber, W. HTSeq—A Python Framework to Work with High-Throughput Sequencing Data. *Bioinformatics* **2015**, *31*, 166–169. [[CrossRef](#)]
36. Love, M.I.; Huber, W.; Anders, S. Moderated Estimation of Fold Change and Dispersion for RNA-Seq Data with DESeq2. *Genome Biol.* **2014**, *15*, 550. [[CrossRef](#)]
37. Chen, C.; Chen, H.; Zhang, Y.; Thomas, H.R.; Frank, M.H.; He, Y.; Xia, R. TBtools: An Integrative Toolkit Developed for Interactive Analyses of Big Biological Data. *Mol. Plant* **2020**, *13*, 1194–1202. [[CrossRef](#)]
38. Lawrence, M.; Huber, W.; Pagès, H.; Aboyoun, P.; Carlson, M.; Gentleman, R.; Morgan, M.T.; Carey, V.J. Software for Computing and Annotating Genomic Ranges. *PLoS Comput. Biol.* **2013**, *9*, e1003118. [[CrossRef](#)]
39. Kolde, R. Pheatmap: Pretty Heatmaps. *R Package Version* **2012**, *1*, 726.
40. Tian, T.; Liu, Y.; Yan, H.; You, Q.; Yi, X.; Du, Z.; Xu, W.; Su, Z. AgriGO v2.0: A GO Analysis Toolkit for the Agricultural Community, 2017 Update. *Nucleic Acids Res.* **2017**, *45*, W122–W129. [[CrossRef](#)]
41. Wu, T.; Hu, E.; Xu, S.; Chen, M.; Guo, P.; Dai, Z.; Feng, T.; Zhou, L.; Tang, W.; Zhan, L.; et al. ClusterProfiler 4.0: A Universal Enrichment Tool for Interpreting Omics Data. *Innovation* **2021**, *2*, 100141. [[CrossRef](#)] [[PubMed](#)]
42. Ramírez, F.; Ryan, D.P.; Grüning, B.; Bhardwaj, V.; Kilpert, F.; Richter, A.S.; Heyne, S.; Dündar, F.; Manke, T. deepTools2: A next generation web server for deep-sequencing data analysis. *Nucleic Acids Res.* **2016**, *44*, W160–W165. [[CrossRef](#)] [[PubMed](#)]
43. Li, H.; Durbin, R. Fast and Accurate Short Read Alignment with Burrows-Wheeler Transform. *Bioinformatics* **2009**, *25*, 1754–1760. [[CrossRef](#)]
44. Koboldt, D.C.; Chen, K.; Wylie, T.; Larson, D.E.; McLellan, M.D.; Mardis, E.R.; Weinstock, G.M.; Wilson, R.K.; Ding, L. VarScan: Variant Detection in Massively Parallel Sequencing of Individual and Pooled Samples. *Bioinformatics* **2009**, *25*, 2283–2285. [[CrossRef](#)]

45. Nguyen, N.H.; Kim, J.H.; Kwon, J.; Jeong, C.Y.; Lee, W.; Lee, D.; Hong, S.-W.; Lee, H. Characterization of Arabidopsis Thaliana FLAVONOL SYNTHASE 1 (FLS1) -Overexpression Plants in Response to Abiotic Stress. *Plant Physiol. Biochem.* **2016**, *103*, 133–142. [[CrossRef](#)] [[PubMed](#)]
46. Ji, X.-R.; Yu, Y.-H.; Ni, P.-Y.; Zhang, G.-H.; Guo, D.-L. Genome-Wide Identification of Small Heat-Shock Protein (HSP20) Gene Family in Grape and Expression Profile during Berry Development. *BMC Plant Biol.* **2019**, *19*, 433. [[CrossRef](#)] [[PubMed](#)]
47. Neta-Sharir, I.; Isaacson, T.; Lurie, S.; Weiss, D. Dual Role for Tomato Heat Shock Protein 21: Protecting Photosystem II from Oxidative Stress and Promoting Color Changes during Fruit Maturation. *Plant Cell* **2005**, *17*, 1829–1838. [[CrossRef](#)]
48. Guo, M.; Liu, J.-H.; Ma, X.; Zhai, Y.-F.; Gong, Z.-H.; Lu, M.-H. Genome-Wide Analysis of the Hsp70 Family Genes in Pepper (*Capsicum Annuum* L.) and Functional Identification of CaHsp70-2 Involvement in Heat Stress. *Plant Sci.* **2016**, *252*, 246–256. [[CrossRef](#)]
49. Abbas, M.; Peszlen, I.; Shi, R.; Kim, H.; Katahira, R.; Kafle, K.; Xiang, Z.; Huang, X.; Min, D.; Mohamadamin, M.; et al. Involvement of CesaA4, CesaA7-A/B and CesaA8-A/B in Secondary Wall Formation in Populus Trichocarpa Wood. *Tree Physiol.* **2020**, *40*, 73–89. [[CrossRef](#)]
50. Zhang, Z.-B.; Zhu, J.; Gao, J.-F.; Wang, C.; Li, H.; Li, H.; Zhang, H.-Q.; Zhang, S.; Wang, D.-M.; Wang, Q.-X.; et al. Transcription Factor AtMYB103 Is Required for Anther Development by Regulating Tapetum Development, Callose Dissolution and Exine Formation in Arabidopsis: Molecular Cloning and Functional Analysis of AtMYB103. *Plant J.* **2007**, *52*, 528–538. [[CrossRef](#)]
51. Stracke, R.; Jahns, O.; Keck, M.; Tohge, T.; Niehaus, K.; Fernie, A.R.; Weisshaar, B. Analysis of PRODUCTION OF FLAVONOL GLYCOSIDES-dependent Flavonol Glycoside Accumulation in Arabidopsis Thaliana Plants Reveals MYB11-, MYB12- and MYB111-independent Flavonol Glycoside Accumulation. *New Phytol.* **2010**, *188*, 985–1000. [[CrossRef](#)] [[PubMed](#)]
52. Gonzalez, A.; Zhao, M.; Leavitt, J.M.; Lloyd, A.M. Regulation of the Anthocyanin Biosynthetic Pathway by the TTG1/BHLH/Myb Transcriptional Complex in Arabidopsis Seedlings. *Plant J.* **2008**, *53*, 814–827. [[CrossRef](#)] [[PubMed](#)]
53. Li, S.; Fu, Q.; Chen, L.; Huang, W.; Yu, D. Arabidopsis Thaliana WRKY25, WRKY26, and WRKY33 Coordinate Induction of Plant Thermotolerance. *Planta* **2011**, *233*, 1237–1252. [[CrossRef](#)]
54. Ishizaki, T.; Maruyama, K.; Obara, M.; Fukutani, A.; Yamaguchi-Shinozaki, K.; Ito, Y.; Kumashiro, T. Expression of Arabidopsis DREB1C Improves Survival, Growth, and Yield of Upland New Rice for Africa (NERICA) under Drought. *Mol. Breed.* **2013**, *31*, 255–264. [[CrossRef](#)]
55. Li, F.; Min, D.; Ren, C.; Dong, L.; Shu, P.; Cui, X.; Zhang, X. Ethylene Altered Fruit Cuticular Wax, the Expression of Cuticular Wax Synthesis-Related Genes and Fruit Quality during Cold Storage of Apple (*Malus Domestica* Borkh. c.v. Starkrimson) Fruit. *Postharvest Biol. Technol.* **2019**, *149*, 58–65. [[CrossRef](#)]
56. Biswal, A.K.; Hao, Z.; Pattathil, S.; Yang, X.; Winkeler, K.; Collins, C.; Mohanty, S.S.; Richardson, E.A.; Gelineo-Albersheim, I.; Hunt, K.; et al. Downregulation of GAUT12 in Populus Deltoides by RNA Silencing Results in Reduced Recalcitrance, Increased Growth and Reduced Xylan and Pectin in a Woody Biofuel Feedstock. *Biotechnol. Biofuels* **2015**, *8*, 41. [[CrossRef](#)]
57. Deng, J.; Wu, D.; Shi, J.; Balfour, K.; Wang, H.; Zhu, G.; Liu, Y.; Wang, J.; Zhu, Z. Multiple MYB Activators and Repressors Collaboratively Regulate the Juvenile Red Fading in Leaves of Sweetpotato. *Front. Plant Sci.* **2020**, *11*, 941. [[CrossRef](#)]
58. Liu, Z.; Running, M.P.; Meyerowitz, E.M. TSO1 Functions in Cell Division during Arabidopsis Flower Development. *Development* **1997**, *124*, 665–672. [[CrossRef](#)]
59. Bajaj, R.; Huang, Y.; Gebrechristos, S.; Mikolajczyk, B.; Brown, H.; Prasad, R.; Varma, A.; Bushley, K.E. Transcriptional Responses of Soybean Roots to Colonization with the Root Endophytic Fungus Piriformospora Indica Reveals Altered Phenylpropanoid and Secondary Metabolism. *Sci. Rep.* **2018**, *18*, 10227. [[CrossRef](#)]
60. Wagner, T.A.; Kohorn, B.D. Wall-Associated Kinases Are Expressed throughout Plant Development and Are Required for Cell Expansion. *Plant Cell* **2001**, *13*, 303–318. [[CrossRef](#)]
61. Le Hir, R.; Sorin, C.; Chakraborti, D.; Moritz, T.; Schaller, H.; Tellier, F.; Robert, S.; Morin, H.; Bako, L.; Bellini, C. ABCG9, ABCG11 and ABCG14 ABC Transporters Are Required for Vascular Development in Arabidopsis. *Plant J.* **2013**, *76*, 811–824. [[CrossRef](#)]
62. Lima, J.E.; Kojima, S.; Takahashi, H.; Von Wirén, N. Ammonium Triggers Lateral Root Branching in Arabidopsis in an AMMONIUM TRANSPORTER1;3-Dependent Manner. *Plant Cell* **2010**, *22*, 3621–3633. [[CrossRef](#)] [[PubMed](#)]
63. Chiang, Y.-H.; Zubo, Y.O.; Tapken, W.; Kim, H.J.; Lavanway, A.M.; Howard, L.; Pilon, M.; Kieber, J.J.; Schaller, G.E. Functional Characterization of the GATA Transcription Factors GNC and CGA1 Reveals Their Key Role in Chloroplast Development, Growth, and Division in Arabidopsis. *Plant Physiol.* **2012**, *160*, 332–348. [[CrossRef](#)] [[PubMed](#)]
64. Zhang, S.; Pan, Y.; Tian, W.; Dong, M.; Zhu, H.; Luan, S.; Li, L. Arabidopsis CNGC14 Mediates Calcium Influx Required for Tip Growth in Root Hairs. *Mol. Plant* **2017**, *10*, 1004–1006. [[CrossRef](#)] [[PubMed](#)]
65. Gao, Y.; Long, R.; Kang, J.; Wang, Z.; Zhang, T.; Sun, H.; Li, X.; Yang, Q. Comparative Proteomic Analysis Reveals That Antioxidant System and Soluble Sugar Metabolism Contribute to Salt Tolerance in Alfalfa (*Medicago Sativa* L.) Leaves. *J. Proteome Res.* **2018**, *18*, 191–203. [[CrossRef](#)]
66. Castro-Rodríguez, R.; Escudero, V.; Reguera, M.; Gil-Díez, P.; Quintana, J.; Prieto, R.I.; Kumar, R.K.; Brear, E.; Grillet, L.; Wen, J.; et al. Medicago Truncatula Yellow Stripe-Like7 Encodes a Peptide Transporter Participating in Symbiotic Nitrogen Fixation. *Plant Cell Environ.* **2021**, *44*, 1908–1920. [[CrossRef](#)]
67. Dash, M.; Yordanov, Y.S.; Georgieva, T.; Tschaplinski, T.J.; Yordanova, E.; Busov, V. Poplar Ptab ZIP 1-like Enhances Lateral Root Formation and Biomass Growth under Drought Stress. *Plant J.* **2017**, *89*, 692–705. [[CrossRef](#)]

68. Ma, H.; Liu, C.; Li, Z.; Ran, Q.; Xie, G.; Wang, B.; Fang, S.; Chu, J.; Zhang, J. ZmbZIP4 Contributes to Stress Resistance in Maize by Regulating ABA Synthesis and Root Development. *Plant Physiol.* **2018**, *178*, 753–770. [[CrossRef](#)]
69. Han, X.; Zhang, M.; Yang, M.; Hu, Y. Arabidopsis JAZ Proteins Interact with and Suppress RHD6 Transcription Factor to Regulate Jasmonate-Stimulated Root Hair Development. *Plant Cell* **2020**, *32*, 1049–1062. [[CrossRef](#)]
70. Peer, W.A.; Hosein, F.N.; Bandyopadhyay, A.; Makam, S.N.; Otegui, M.S.; Lee, G.-J.; Blakeslee, J.J.; Cheng, Y.; Titapiwatanakun, B.; Yakubov, B.; et al. Mutation of the Membrane-Associated M1 Protease APM1 Results in Distinct Embryonic and Seedling Developmental Defects in *Arabidopsis*. *Plant Cell* **2009**, *21*, 1693–1721. [[CrossRef](#)]
71. Demirkol, G. PopW Enhances Drought Stress Tolerance of Alfalfa via Activating Antioxidative Enzymes, Endogenous Hormones, Drought Related Genes and Inhibiting Senescence Genes. *Plant Physiol. Biochem.* **2021**, *166*, 540–548. [[CrossRef](#)] [[PubMed](#)]
72. Satoh, R.; Fujita, Y.; Nakashima, K.; Shinozaki, K.; Yamaguchi-Shinozaki, K. A Novel Subgroup of BZIP Proteins Functions as Transcriptional Activators in Hypoosmolarity-Responsive Expression of the ProDH Gene in *Arabidopsis*. *Plant Cell Physiol.* **2004**, *45*, 309–317. [[CrossRef](#)]
73. Park, S.-Y.; Grabau, E. Bypassing miRNA-Mediated Gene Regulation under Drought Stress: Alternative Splicing Affects CSD1 Gene Expression. *Plant Mol. Biol.* **2017**, *95*, 243–252. [[CrossRef](#)]
74. Vanani, F.R.; Shabani, L.; Sabzalain, M.R.; Dehghanian, F.; Winner, L. Comparative Physiological and Proteomic Analysis Indicates Lower Shock Response to Drought Stress Conditions in a Self-Pollinating Perennial Ryegrass. *PLoS ONE* **2020**, *15*, e0234317. [[CrossRef](#)] [[PubMed](#)]
75. Sow, M.D.; Le Gac, A.; Fichot, R.; Lanciano, S.; Delaunay, A.; Le Jan, I.; Lesage-Descauses, M.; Citerne, S.; Caius, J.; Brunaud, V.; et al. RNAi Suppression of DNA Methylation Affects the Drought Stress Response and Genome Integrity in Transgenic Poplar. *New Phytol.* **2021**, *232*, 80–97. [[CrossRef](#)] [[PubMed](#)]
76. Yang, M.; Yang, Q.; Fu, T.; Zhou, Y. Overexpression of the Brassica Napus BnLAS Gene in *Arabidopsis* Affects Plant Development and Increases Drought Tolerance. *Plant Cell Rep.* **2011**, *30*, 373–388. [[CrossRef](#)] [[PubMed](#)]
77. Banerjee, A.K.; Lin, T.; Hannapel, D.J. Untranslated Regions of a Mobile Transcript Mediate RNA Metabolism. *Plant Physiol.* **2009**, *151*, 1831–1843. [[CrossRef](#)]
78. Ham, B.-K.; Brandom, J.L.; Xoconostle-Cázares, B.; Ringgold, V.; Lough, T.J.; Lucas, W.J. A Polypyrimidine Tract Binding Protein, Pumpkin RBP50, Forms the Basis of a Phloem-Mobile Ribonucleoprotein Complex. *Plant Cell* **2009**, *21*, 197–215. [[CrossRef](#)]
79. Haywood, V.; Yu, T.-S.; Huang, N.-C.; Lucas, W.J. Phloem Long-Distance Trafficking of *GIBBERELLIC ACID-INSENSITIVE* RNA Regulates Leaf Development: Phloem Delivery of RNA Regulates Leaf Development. *Plant J.* **2005**, *42*, 49–68. [[CrossRef](#)]
80. Kim, M.; Canio, W.; Kessler, S.; Sinha, N. Developmental Changes Due to Long-Distance Movement of a Homeobox Fusion Transcript in Tomato. *Sci. New Ser.* **2001**, *293*, 287–289. [[CrossRef](#)]
81. Ruiz-Medrano, R.; Xoconostle-Cázares, B.; Lucas, W.J. Phloem Long-Distance Transport of CmNACP mRNA: Implications for Supracellular Regulation in Plants. *Development* **1999**, *126*, 4405–4419. [[CrossRef](#)] [[PubMed](#)]
82. Reina-Pinto, J.J.; Voisin, D.; Kurdyukov, S.; Faust, A.; Haslam, R.P.; Michaelson, L.V.; Efremova, N.; Franke, B.; Schreiber, L.; Napier, J.A.; et al. Misexpression of FATTY ACID ELONGATION1 in the *Arabidopsis* Epidermis Induces Cell Death and Suggests a Critical Role for Phospholipase A2 in This Process. *Plant Cell* **2009**, *21*, 1252–1272. [[CrossRef](#)] [[PubMed](#)]
83. Ye, H.; Liu, S.; Tang, B.; Chen, J.; Xie, Z.; Nolan, T.M.; Jiang, H.; Guo, H.; Lin, H.-Y.; Li, L.; et al. RD26 Mediates Crosstalk between Drought and Brassinosteroid Signalling Pathways. *Nat. Commun.* **2017**, *8*, 14573. [[CrossRef](#)]
84. Zhao, C.; Zayed, O.; Yu, Z.; Jiang, W.; Zhu, P.; Hsu, C.-C.; Zhang, L.; Tao, W.A.; Lozano-Durán, R.; Zhu, J.-K. Leucine-Rich Repeat Extensin Proteins Regulate Plant Salt Tolerance in *Arabidopsis*. *Proc. Natl. Acad. Sci. USA* **2018**, *115*, 13123–13128. [[CrossRef](#)] [[PubMed](#)]
85. Kim, S.; Kang, J.; Cho, D.-I.; Park, J.H.; Kim, S.Y. ABF2, an ABRE-Binding BZIP Factor, Is an Essential Component of Glucose Signaling and Its Overexpression Affects Multiple Stress Tolerance: ABF2 Is a Positive Component of Glucose Signaling. *Plant J.* **2004**, *40*, 75–87. [[CrossRef](#)] [[PubMed](#)]
86. Dheilly, E.; Gall, S.L.; Guillou, M.-C.; Renou, J.-P.; Bonnin, E.; Orsel, M.; Lahaye, M. Cell Wall Dynamics during Apple Development and Storage Involves Hemicellulose Modifications and Related Expressed Genes. *BMC Plant Biol.* **2016**, *16*, 201. [[CrossRef](#)] [[PubMed](#)]
87. Vaahtera, L.; Schulz, J.; Hamann, T. Cell Wall Integrity Maintenance during Plant Development and Interaction with the Environment. *Nat. Plants* **2019**, *5*, 924–932. [[CrossRef](#)]
88. Qiu, D.; Xu, S.; Wang, Y.; Zhou, M.; Hong, L. Primary Cell Wall Modifying Proteins Regulate Wall Mechanics to Steer Plant Morphogenesis. *Front. Plant Sci.* **2021**, *12*, 751372. [[CrossRef](#)]
89. Shimmen, T. The Sliding Theory of Cytoplasmic Streaming: Fifty Years of Progress. *J. Plant Res.* **2007**, *120*, 31–43. [[CrossRef](#)]
90. Karim, S.K.A.; Allan, A.C.; Schaffer, R.J.; David, K.M. Cell Division Controls Final Fruit Size in Three Apple (*Malus x Domestica*) Cultivars. *Horticulturae* **2022**, *8*, 657. [[CrossRef](#)]
91. Gillaspay, G.; Ben-David, H.; Gruissem, W. Fruits: A Developmental Perspective. *Plant Cell* **1993**, *5*, 1439. [[CrossRef](#)] [[PubMed](#)]
92. Yang, X.Y.; Wang, Y.; Jiang, W.J.; Liu, X.L.; Zhang, X.M.; Yu, H.J.; Huang, S.W.; Liu, G.Q. Characterization and Expression Profiling of Cucumber Kinesin Genes during Early Fruit Development: Revealing the Roles of Kinesins in Exponential Cell Production and Enlargement in Cucumber Fruit. *J. Exp. Bot.* **2013**, *64*, 4541–4557. [[CrossRef](#)] [[PubMed](#)]
93. Onelli, E.; Idilli, A.I.; Moscatelli, A. Emerging Roles for Microtubules in Angiosperm Pollen Tube Growth Highlight New Research Cues. *Front. Plant Sci.* **2015**, *6*, 51. [[CrossRef](#)] [[PubMed](#)]

94. Qaseem, M.F.; Wu, A.-M. Balanced Xylan Acetylation Is the Key Regulator of Plant Growth and Development, and Cell Wall Structure and for Industrial Utilization. *IJMS* **2020**, *21*, 7875. [[CrossRef](#)]
95. Bath, R.; Nicolle, C.; Cuciurean, I.S.; Simonsen, H.T. Biosynthesis and Industrial Production of Androsteroids. *Plants* **2020**, *9*, 1144. [[CrossRef](#)]
96. Lombardo, V.A.; Osorio, S.; Borsani, J.; Lauxmann, M.A.; Bustamante, C.A.; Budde, C.O.; Andreo, C.S.; Lara, M.V.; Fernie, A.R.; Drincovich, M.F. Metabolic Profiling during Peach Fruit Development and Ripening Reveals the Metabolic Networks That Underpin Each Developmental Stage. *Plant Physiol.* **2011**, *157*, 1696–1710. [[CrossRef](#)]
97. Torres, C.A.; Azocar, C.; Ramos, P.; Pérez-Díaz, R.; Sepulveda, G.; Moya-León, M.A. Photooxidative Stress Activates a Complex Multigenic Response Integrating the Phenylpropanoid Pathway and Ethylene, Leading to Lignin Accumulation in Apple (*Malus Domestica* Borkh.) Fruit. *Hortic. Res.* **2020**, *7*, 22. [[CrossRef](#)]
98. Stintzi, A.; Weber, H.; Reymond, P.; Browse, J.; Farmer, E.E. Plant Defense in the Absence of Jasmonic Acid: The Role of Cyclopentenones. *Proc. Natl. Acad. Sci. USA* **2001**, *98*, 12837–12842. [[CrossRef](#)]
99. Zeb, A. Concept, mechanism, and applications of phenolic antioxidants in foods. *J. Food Biochem.* **2020**, *44*, e13394. [[CrossRef](#)]
100. Treutter, D. Biosynthesis of Phenolic Compounds and Its Regulation in Apple. *Plant Growth Regul.* **2001**, *34*, 71–89. [[CrossRef](#)]
101. Ma, L.; He, J.; Liu, H.; Zhou, H. The Phenylpropanoid Pathway Affects Apple Fruit Resistance to *Botrytis Cinerea*. *J. Phytopathol.* **2018**, *166*, 206–215. [[CrossRef](#)]
102. Francini, A.; Sebastiani, L. Phenolic Compounds in Apple (*Malus x Domestica* Borkh.): Compounds Characterization and Stability during Postharvest and after Processing. *Antioxidants* **2013**, *2*, 181–193. [[CrossRef](#)] [[PubMed](#)]
103. Li, P.; Cheng, L. The elevated anthocyanin level in the shaded peel of ‘Anjou’ pear enhances its tolerance to high temperature under high light. *Plant Sci.* **2009**, *177*, 418–426. [[CrossRef](#)]
104. Hu, Y.; Cheng, H.; Zhang, Y.; Zhang, J.; Niu, S.; Wang, X.; Li, W.; Zhang, J.; Yao, Y. The MdMYB16/MdMYB1-miR7125-MdCCR Module Regulates the Homeostasis between Anthocyanin and Lignin Biosynthesis during Light Induction in Apple. *New Phytol* **2021**, *231*, 1105–1122. [[CrossRef](#)]
105. Liu, X.; Zhao, C.; Gao, Y.; Xu, Y.; Wang, S.; Li, C.; Xie, Y.; Chen, P.; Yang, P.; Yuan, L.; et al. A Multifaceted Module of BRI1 ETHYLMETHANE SULFONATE SUPPRESSOR1 (BES1)-MYB88 in Growth and Stress Tolerance of Apple. *Plant Physiol.* **2021**, *185*, 1903–1923. [[CrossRef](#)] [[PubMed](#)]
106. Bajguz, A.; Chmur, M.; Gruszka, D. Comprehensive Overview of the Brassinosteroid Biosynthesis Pathways: Substrates, Products, Inhibitors, and Connections. *Front. Plant Sci.* **2020**, *11*, 1034. [[CrossRef](#)] [[PubMed](#)]
107. Thieme, C.J.; Rojas-Triana, M.; Stecyk, E.; Schudoma, C.; Zhang, W.; Yang, L.; Miñambres, M.; Walther, D.; Schulze, W.X.; Paz-Ares, J.; et al. Endogenous Arabidopsis Messenger RNAs Transported to Distant Tissues. *Nat. Plants* **2015**, *1*, 15025. [[CrossRef](#)]
108. Zhang, W.-N.; Gong, L.; Ma, C.; Xu, H.-Y.; Hu, J.-F.; Harada, T.; Li, T.-Z. Gibberellic Acid-Insensitive mRNA Transport in Pyrus. *Plant Mol. Biol. Rep.* **2012**, *30*, 614–623. [[CrossRef](#)]
109. Xu, H.; Zhang, W.; Li, M.; Harada, T.; Han, Z.; Li, T. Gibberellic Acid Insensitive mRNA Transport in Both Directions between Stock and Scion in Malus. *Tree Genet. Genomes* **2010**, *6*, 1013–1019. [[CrossRef](#)]
110. Xu, H.; Iwashiro, R.; Li, T.; Harada, T. Long-Distance Transport of Gibberellic Acid Insensitive mRNA in Nicotiana Benthiana. *BMC Plant Biol.* **2013**, *13*, 165. [[CrossRef](#)]
111. Zhang, W.N.; Duan, X.W.; Ma, C.; Harada, T.; Li, T.Z. Transport of mRNA Molecules Coding NAC Domain Protein in Grafted Pear and Transgenic Tobacco. *Biol. Plant.* **2013**, *57*, 224–230. [[CrossRef](#)]
112. Xia, C.; Zheng, Y.; Huang, J.; Zhou, X.; Li, R.; Zha, M.; Wang, S.; Huang, Z.; Lan, H.; Turgeon, R.; et al. Elucidation of the Mechanisms of Long-Distance mRNA Movement in a *Nicotiana Benthiana* /Tomato Heterograft System. *Plant Physiol.* **2018**, *177*, 745–758. [[CrossRef](#)] [[PubMed](#)]